STUDY OF 1-DIMENSIONAL MOVEMENT OF LAMBDA DNA IN NANOCHANNELS

SARABJIT SINGH

NATIONAL UNIVERSITY OF SINGAPORE

2014

STUDY OF 1-DIMENSIONAL MOVEMENT OF LAMBDA DNA IN NANOCHANNELS

SARABJIT SINGH

(M.Ed), NTU

A THESIS SUBMITTED

FOR THE DEGREE OF MASTERS OF SCIENCE (RESEARCH)

DEPARTMENT OF PHYSICS

NATIONAL UNIVERSITY OF SINGAPORE

2014

DECLARATION

I hereby declare that the thesis is my original work and it has been written by me in its entirety.

I have duly acknowledged all the sources of information which have been used in the thesis.

This thesis has also not been submitted for any degree in any university previously.

Sarabjit Singh

3 January 2014

Acknowledgements

First, I would like to thank Associate Professor Johan R. C. van der Maarel for allowing me the opportunity to investigate the interesting physics involved in single molecules. Single molecule techniques impact optics, electronics, and biology. The inter and intra disciplinary approach bring with it many challenges and possibilities. The promise of single molecule in vitro imaging brings with it an enormous potential in allowing for devices to be fabricated to mimic environments to directly observe biomolecules in their native process.

Last, but not least, I would like my wife Jasmin, daughter Keerat and son Brahmjot for reminding me that there are other joys in life other than research.

Table of Contents

Summary

This report demonstrates how PDMS casting can be used to investigate fluorescence labelled single Lambda DNA molecules. Analysis of the mean squared displacement data showed a diffusion slope during the first few seconds. At later time's entropic trapping effect of the DNA in channel leads to an elastic response so that the MSD levels off to a constant value. Additionally, comparisons of diffusions coefficients to the extension of DNA molecules agree with predicted revisiting blob theory.

List of figures

List of tables

Chapter 1 Introduction to report

This chapter includes a short introduction of the study on single DNA molecules. The gaps in traditional methods are discussed leading to the proposed method of investigation of single DNA molecules that is used in this report.

1.1 Purpose of study

Deoxyribonucleic Acid (DNA) is a long biopolymer made from repeating units called nucleotides, encoding the genetic instruction used in the development and functioning of all known living organisms and many viruses. Single molecule studies of the movement of DNA are important in a variety of biological or biotechnology process, for example, in the development of nanoparticles for genome analysis. It is also a critical research topic, which will be explored more in this report, specifically in the area of research of configuration and dynamics of a flexible chain confined in a narrow tube.

Experiments for determining the movement of a single DNA molecule have been explored over decades and several theories have been proposed to explain the dynamics of a single DNA molecule. However, in the past with traditional experimental techniques, it is difficult meet the requirements of the observation and recording of the movement of a single DNA molecule in the physiological range. Nowadays with the development of more advanced experimental techniques, a single DNA molecule can be observed by first labelling with a dye and next imaging under a fluorescence microscope.

Another major advancement is through the development of microfluidic and nanofluidic structures. To illustrate, a nanofluidic channel can be assembled using polydimethylsiloxane (PDMS) scaffolding by fabrication on silicon wafers. With micro or nanofluidic devices, the sample volume can be reduced to a few microliters, substantially reducing the cost of running an assay. Such novel methods can offer a one-dimension confinement in which the single DNA molecule would be allowed to move freely. Thus several interesting results, which will be explored further in this report, can be obtained from such one-dimension movement physics.

Random movements of a single molecule can be described by statistical mechanics using the concept of mean squared displacement. Further, applied theories have been developed to describe the configuration and dynamics of DNA molecules in nanochannels. Within them is the important blob theory developed by De Gennes which has since been widely accepted and proven to be reliable by the huge body of research.

1.2 Conclusion

The main focus of this report is to investigate the one dimensional movement of Lambda DNA molecules in three different TE buffer concentrations while confined in two channel dimensions.

Chapter 2 Background theory

This chapter included background introduction on the topics that is pertinent to this report. It includes the literature review of what has been investigated previously and the limitation and gaps that will be address in this report.

2.1 DNA and fluorescent dye

This section introduces the topic of DNA and fluorescence beads.

2.1.1 DNA

Watson and Crick first published the structure of deoxyribonucleic acid (DNA) in the April edition of Nature back in 1953. It was the first publication that described the double helical structure of DNA.

DNA is a long polymer chain made up of repeating units called nucleotides. In most DNA there are two nucleotide chains that twist around each other to form a double helix structure that Watson and Crick observed. The two helical chains are each coiled round the same axis and each has a pitch of 34 Å and a radius of 10 Å about the central axis. The stability of double stranded DNA (dsDNA) form depends not only on the G-C content (% G-C basepairs) but also on the sequence (since stacking is sequence specific) and length (as longer molecules tend to be more stable). The persistence length

of dsDNA is ~50 nm. The two chains are very stable, held together by hydrogen bonds between base-pairs (bps). This stability is very important as it allows for the transfer of genetic material through generations with little genetic drift and low error rates as evident through evolution.

The four bases (called nucleobases) found in DNA are Adenine, Thymine, Cytosine and Guanine (abbreviated as A, T, C and G). The backbone of the DNA is made of alternating sugars (called deoxyribose) and phosphate groups, with the four bases attached to the sugar. These nucleobases are classified under two types: the purines and pyrimidines. The purines include the bases adenine and guanine, and are fused by five and six membered heterocyclic compounds respectively. The pyrimidines are six membered rings of the bases cytosine and thymine. Both these types are based on carbon-based rings with nitrogen atom substitutions. The pyrimidines being single ringed while the purines being double rings of five and six atoms fused together, where two carbon atoms are shared between the rings.

In a DNA double helix, each type of nucleobase from one strand bonds with just one type of nucleobase on the other strand. This is importantly called complimentary base pairing. Here, purines form hydrogen bonds to pyrimidines, with adenine bonding to thymine from the opposite nucleotide chain with two hydrogen bonds, and cytosine bonding to guanine with three hydrogen bonds. As hydrogen bonds are weaker than covalent bonds, they can be broken and re-bonded easily. In this regard the two nucleotide strands of DNA in a double helix can be pulled apart like an ordinary zipper, either by a mechanical force or when heated to high temperatures. As, a result of this complementarity base pairing, all the information in the double-stranded sequence of a DNA helix is duplicated on each strand, which is vital in DNA replication. The two types of base pairs form different numbers of hydrogen bonds. Remember, while adenine and thymine form just two

hydrogen bonds between them, cytosine and guanine forms three hydrogen bonds between them. This additional hydrogen bond gives rise to a binding energy difference of around 2 kT [1], allowing discrimination in energetic terms as well as structural differences between the letters (A, T, C & G) in the genetic code. Additionally, it can be expected that DNA with a higher number of G-C bases to be more stable than another with lower number of G-C bases.

Another important property of DNA is that each phosphate group in the backbone of DNA can carry a negative charge in moderate pH buffer solution. Moreover, these charges can result in electrostatic repulsions between nucleotides and thus lead to local stiffening of the backbone. However, in the typical DNA biological storage buffer solution, these electrostatic interactions decay over a small length scale due to the high salt concentration of the storage buffer. In consequence, these interactions do not contribute significantly to the stiffness of the DNA while in storage buffer. However, little is known on the dynamics of a single DNA molecule under different buffer conditions.

2.1.2 Fluorescence process and fluorescence beads

When a fluorescent chemical compound (called fluorophore) is irradiated by light of a particular wavelength, upon absorbing this incident light, it will result in an energy level transition, see fig2.1.2 below. At higher energy levels, the fluorophore will disperse the energy radioactively or emit light at a longer wavelength [6]. This emitted light can then be detected by a fluorescent microscope. The quantum yield is an indication of the efficiency of the dye, and the extinction coefficient is the amount of light that can be absorbed by a fluorophore. For each fluorophore both the quantum yield and extinction coefficient are specific and when multiplied together calculates the brightness of the fluorescent molecule. Therefore, fluorophores can be used as dyes for biological molecules

since the emission light at a particular wavelength can be observed directly by an optical objective. An example of a fluorescence bead which can be illuminated because of such fluorscene phenomenon is YOYO-1.

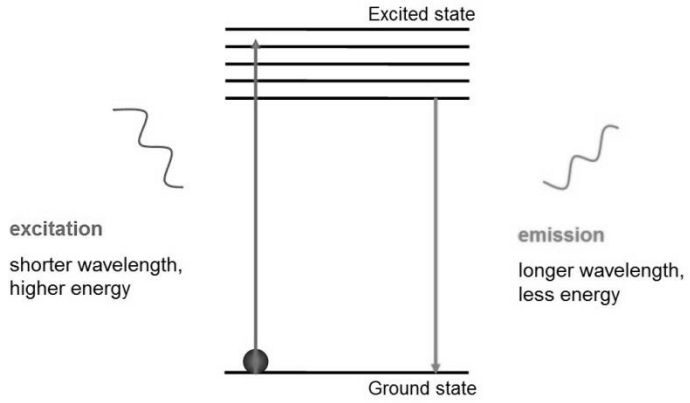

Fig 2.1.2 Energy level transition

This ability to attach a fluorophore to a single molecule allows for the investigation into the dynamics of a single DNA molecule.

2.1.3 YOYO-1

Single-molecule fluorescence microscopy has been an extremely versatile tool used to explore the statistical-mechanical properties of DNA duplex [2]. YOYO-1 is a green fluorescent dye often used for single DNA imaging and is one of the highly sensitive fluorescent probes currently available.

When bound to DNA, it will exhibit a 100- to 1000-fold fluorescent enhancement. With the help of this phenomenon, labelled single DNA can be easily imaged and investigated. When bound to DNA, YOYO-1 can be excited by blue wavelength light (491 nm) and will emit a green wavelength light (502 nm). The importance of a different maximum wavelength for the excitation and emission light is critical to allow for a direct measure of the molecule under investigation. Otherwise the brighter incident light overwhelms the weaker emitted fluorescence light. Any overlap in the excitation and emission intensities and wavelength can be further eliminated by filters in the fluorescence microscope. Compared to other nucleic acid-specific dyes such as BODAPI, YOYO-1's high brightness and relative photostability make it an excellent choice for single DNA mapping [3-5].

2.2 DNA model

The DNA can be modelled as a simple polymer. In polymer physics, the physical properties involved in the molecular mechanics can be described by only these three parameters [7]:

- Contour length, L,
- Persistence length, L_p and
- Effective width, ω_{eff}.

The contour length is the total length of the DNA molecule at maximum physically possible extension. Each base-pair contribution contributes a 0.34 nm segment to the contour length of the DNA.

DNA in solution does not take a rigid structure but is continually changing conformation due to thermal vibration and collision with buffer molecules. Hence, the persistence length is used to quantifying the stiffness of a polymer. Informally, for pieces of the polymer that are shorter than the persistence length, the molecule behaves rather like a flexible elastic rod, while for pieces of the polymer that are much longer than the persistence length, the properties can only be described statistically like a three dimensional random walk. Formally, the persistence length is defined as the length over which correlations in the direction of the tangent are lost.

The persistence length is also considered to be one half of the Kuhn length (the length of hypothetical segments that the chain can be considered as freely joined). The persistence length equals the average projection of the end-to-end vector on the tangent to the chain contour at a chain end in the limit of infinite chain length.

The intrinsic persistence length of DNA is $L_p = 50$ nm. The intrinsic width of DNA is $\omega_o = 2$ nm. However, due to the molecule interacting with the ion surrounding it, the DNA has an effective width (ω_{eff}), which is much larger than its intrinsic width [8].

2.2.1 Ideal chain model

An ideal chain model (or freely-jointed chain) is the simplest model to describe polymers. It only assumes a polymer as a random walk and neglects any kind of interaction among monomers. Although it is a simple model, it does give you some insight about the physics of polymer.

In this model, monomers are idealised as rigid rods of fixed length l, and their orientation is completely independent of the orientations and position of neighbouring monomers, to the extent that two monomers can co-exist at the same place. In this simple approach where no interactions between monomers are considered, the energy of the polymer is taken to be independent of its shape which means that at thermodynamic equilibrium, all of its shape configurations are equally likely to occur as the polymer fluctuates in time according to Maxwell-Boltzmann distribution.

Let N monomers form the polymer, whose total unfolded length is

$$L = Nl.$$

Let $\vec{R}$ be the total end to end vector of an ideal chain and $\overrightarrow{r_1}, \dots, \overrightarrow{r_N}$ the vectors corresponding to individual monomers. Those random vectors have components in three directions of space. Fig. 2.2.1 below shows a sketch of a short ideal chain.

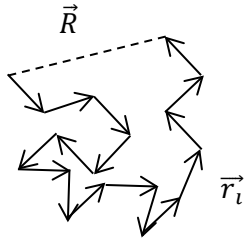

Fig 2.2.1 A short ideal chain

The orientation of one link is independent of the orientation of the neighbouring links, and there is no interaction between segments that are not directly linked together. In addition, there are no long range interactions [9].

The end-to-end distance of the molecule can be calculated from the expectation value of the squared sum of all steps.

$$\langle h^2 \rangle = N l^2$$

This can be used to calculate the effective radius for the polymer coil, which is proportional to the square root of the number of links.

$$R_p \cong \langle h^2 \rangle^{1/2} \cong N^{1/2} l$$

For DNA, this ideal chain model has to be altered because neighbouring base pairs are stacked, resulting in a bending stiffness. The limitation of this model will be addressed next and improved by the worm-like chain model, described in the next section.

2.2.2 Worm-like chain model

The worm-like chain (WLC) model describes the polymer as a uniform and continuously flexible rod.

The directional correlation of the worm-like chain is

$$\langle \cos\theta(s) \rangle = exp\left(-\frac{|s|}{L_p}\right).$$

The persistence length L_p is the typical length scale over which the orientation correlation is lost.

For a small length, $s \ll L_p$, then

$$\langle \cos\theta(s) \rangle = 1 - \frac{1}{2}\langle \theta^2(s) \rangle + \cdots$$

and

$$exp\left(-\frac{s}{L_p}\right) = 1 - \frac{s}{L_p}.$$

Therefore,

$$\langle \theta^2(s) \rangle = 2\frac{s}{L_p}.$$

However if the DNA molecule is confined in a nanochannel then the worm-like model would not be appropriate as it does not consider the effect of the channel walls on the DNA molecule. The next section considers the effect of confinement experienced by a single DNA molecule.

2.2.3 De Gennes's blob model for confined polymer

Consider a DNA molecule of contour length L, width ω and persistence length L_p, which is now confined in a nanochannel of width D that is less than the radius of gyration of the molecule. In molecular physics, the radius of gyration is used to describe the dimension of a polymer chain. When $D \gg L_p$ the molecule is free to coil in the nanochannel and the elongation is entirely due to the excluded volume interaction between segments of the polymer, which are greatly separated in position along the backbone (see fig 2.2.3 below).

De Gennes developed a scaling theory for the average extension of a confined self-avoiding polymer [10-13], which was later generalised by Schafer and Pincus to the case of a persistent self-avoiding polymer [14]. The extension $R_{/\!/}$ scales with D in the following relation, in the De Gennes theory.

$$R_{/\!/} \cong L\left(\frac{\omega L_p}{D^2}\right)^{1/3}$$

If the aspect ratio of the channel is not unity, i.e. the width D_1 does not equal the depth D_2, then the last equation is still valid provided that D is replaced by the geometric average of the dimension

[15]: $D_{av} = \sqrt{D_1 D_2}$. Figure 2.2.3 shows a molecule in the De Gennes regime where the molecule is subdivided equally into blobs with contour length L.

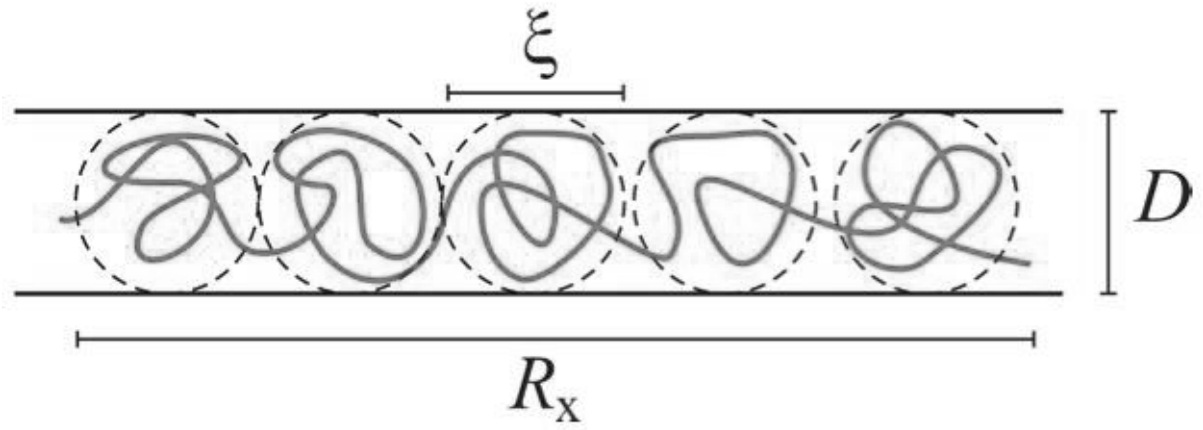

Fig 2.2.3 A confined polymer in the De Gennes regime ($D \gg L_p$)

Thus, the contour length of the DNA molecule within a blob in the De Gennes regime can be represented as a scaling law by using Flory scaling [16].

$$L_{blob} \sim H^{5/3} L_p^{-1/3} \omega^{-1/3}$$

This scaling law is applied to the confines of a nanoslit. Here H is the diameter of the blob and ω is the effective chain width. A single Flory exponent of $3/5$ is used here. The number of the blob is $N_{blob} = L/L_{blob}$, where L is the contour length.

In the Zimm model [17], polymer in each blob is hydrodynamically coupled to its entrained solvent, resulting in a drag force on each blob proportional to H. The resulting scaling of diffusivity is

$$D \sim 1/(N_{blob}H) \sim H^{2/3}L_p^{-1/3}\omega^{-1/3}L^{-1}.$$

This is the diffusivity law derived from classical blob theory [18].

2.3 Micro- and Nanofluidics

This section discusses the advantages of using a micro- and nanofluidic system to study biological molecules. Section 2.1.2 discussed how fluorophore can be used to help in the investigation of single DNA molecules, now let's look at how we can confine these single molecules for investigation into their dynamics.

The small volume and constrained dynamics due to confinement has resulted in greater temporal and spatial resolution. Both the microfluidic and nanofluidic fields are recent, where microfluidics was gaining research popularity in mid 1990s while it was in the year 2000 for nanofluidics. Advances in nanofabrication have made it possible to fabricate quasi one-dimensional devices with cross-sectional diameters on the order of tens to hundred nanometres. These nanochannels serve as a platform for studying, among others, single DNA molecules. [7, 19-25]

Microfluidics systems investigate the behaviour, through the precision and control and manipulation of fluids that are geometrically constrained to a small volume, typically sub-millimetre scale. This is similar for nanofluidics systems except here the structure dimensions are in the nanometre (typically 1-100 nm) range. The region between 100 nm and 1 µm typically falls under either category.

The very small dimensionless quantity, Reynolds number is often used to predict flow patterns in fluid flow situation that can occur in larger microfluidic systems. The Reynolds number defines the ratio of the internal force, momentum of a fluid to viscous forces. If the Reynolds number is very small, fluids flowing through a system side-by-side, not necessarily mixing in the traditional sense. Molecular transporting between the two fluids must often be through diffusion. In micro- and nanofluidic systems, Poiseuille flow is the dominant hydrodynamic mechanism. This implies that the volumetric flow rate, Q of a fluid in a channel is linear with the pressure gradient across the channel [26].

$$Q = \frac{\Delta P}{R_H}$$

The constant of proportionality R_H between flow rates and pressure is known as hydraulic resistance, which is dependent on the viscosity η, total length L, and characteristic width scale a, of the channel.

$$R_H = \frac{\eta L}{a^4}$$

The small sizes associated with micro- and nanofluidic systems suggest a very high hydraulic resistance. The high hydraulic resistance here is an important concept when calculating flow rates based on applied pressure [27-28].

Advances in microfluidic technology are revolutionising molecular biology procedures for enzymatic analysis, DNA analysis and proteomics by microfluidic biochips. The basic idea of microfluidic biochips is to integrate assay operations such as detection, as well as sample pre-treatment and sample preparation on one chip.

In nanofluidic systems, the physical scaling lengths of the fluid coincide more closely with dimensions of the nanostructure itself. Therefore, more physical constraints are placed on the behaviour of the fluid. These physical constraints induce regions of fluid to exhibit new properties not observed in bulk.

In nanofluidic system, electrical double layer is an important characteristic. All electrified interfaces induce an organised charge distribution near the surface. The field from the charged surface may cause dramatic changes in the composition of the fluid and the related properties of fluid motion in the structure. For example, hydrogen atoms in silanol groups on the surface of glass can dissociate, leaving a negative charge. The field through the charged surface affects the ions in the fluid. As a result, ions with opposite charge to the surface are more likely to be found in their vicinity. This ionic behaviour allows electric fields to be used as a driver of fluid through the channel besides the applied pressure. In contrast, the flow if fluid through such a system can result in net electric fields.

Because of the small size of the fluidic conduits, nanofluidic structures are naturally applied in situations demanding that samples be handled in exceedingly small quantities, including Coulter counting, analytical separations and determinations of biomolecules, such as DNA. One of the more promising areas of nanofluidic is its potential for integration into microfluidic systems, i.e. Lab-on-a-chip structures.

While Debye length in a microfluidic system is typically much small than the length scale of the system, they may be comparable in a nanofluidic system. Therefore, some authors characterized nanofluidics as systems having length scales of the Debye length of the fluid, rather than citing an absolute length cut-off [26]. Due to the ionic environment in nanofluidic systems, long range electrostatic interactions between molecules dominate over van der Waals forces [29].

2.4 Mean squared displacement and diffusion coefficient

In statistical mechanics, the mean squared displacement (MSD) is the most common measure of the spatial extent of random motion. In some way it is often enlightening to think of the MSD as the amount of the system 'explored' by the random walker. In this research, the MSD is the key factor that could determine the mode of movement of the particle since the biopolymers often behave as a random walk [30]. MDS is defined as

$$MSD \equiv \langle (x(t) - x_o)^2 \rangle.$$

Where $x(t)$ represents the position of the particle at a certain time x_o represents the initial position of the particle at time $t = 0$.

Now, let's find the relation between the MSD and diffusion coefficient D in one dimensional case.

The probability density function (PDF) for a particle in one dimension is found by solving the one-dimensional diffusion equation, as shown below.

$$\frac{\partial p(x,t|x_o)}{\partial t} = D\,\frac{\partial^2 p(x,t|x_o)}{\partial x^2}$$

Here given the initial conditions $p(x_o, t = 0|x_o) = \delta(x - x_o)$, where $x(t)$ is the position of the particle at a later time while x_o is the initial position of the particle. D is the diffusion coefficient, which is an indirect measure of the particle's speed. The diffusion equation states that the speed at which the probability for finding the particle at $x(t)$ is position dependent.

It can be shown that the one-dimensional PDF solves to

$$P(x,t) = \frac{1}{\sqrt{4\pi Dt}} exp\left(-\frac{(x-x_o)^2}{4Dt}\right).$$

This states that the probability of finding the particle at $x(t)$ is Gaussian, and the wigth of the Gaussian is time dependent. More specifically, the full width at half maximum (FWHM) scales as

$$FWHM \sim \sqrt{t}.$$

This Gaussian function is very useful in the measurement of the MSD. With time increasing, the width of this Gaussian will increase. From the definition of MSD, the equation can be expanded out as the ensemble average

$$\langle (x - x_o)^2 \rangle = \langle x^2 \rangle + x_o^2 - 2x_o \langle x \rangle.$$

To find the MSD, we can find the moment-generating function, an extremely useful term, and the generating function when dealing with probability densities. The moment-generating function describes the k^{th} moment of the PDF. The first moment of the displacement PDF shown above is simply the mean, $\langle x \rangle$. The second moment is given as $\langle x^2 \rangle$. To find the moment-generating function it is convenient to introduce the characteristic equation.

$$G(k) = \langle e^{ikx} \rangle \equiv \int_I e^{ikx} P(x, t|x_o) dx$$

In above equation, the exponential can be expanded to give

$$G(k) = \sum_{m=0}^{\infty} \frac{(ik)^m}{m!} \mu_m.$$

By taking the natural logarithm of the characteristic equation, a new equation, called the Cumulant generating function is obtained.

$$\ln(G(k)) = \sum_{m=1}^{\infty} \frac{(ik)^m}{m!} \kappa_m$$

Here κ_m is the m^{th} cumulant of x.

The first two cumulants are related to the first two moments, μ, via $\kappa_1 = \mu_1$ and $\kappa_2 = \mu_2 - \mu_1^2$, where the second cumulant is the variance, σ^2.

With these definitions accounted for one can investigate the moments of the Brownian particle probability density function.

$$G(k) = \frac{1}{\sqrt{4\pi D t}} \int_I \exp(ikx) \exp\left(-\frac{(x - x_o)^2}{4Dt}\right) dx$$

By completing the square and knowing the total area of the Gaussian one arrives at

$$G(k) = \exp(ikx - \kappa^2 Dt).$$

Taking the lateral logarithms on both sides and comparing the powers of ik to the cumulant generating function above, the first cumulant is then

$$\kappa_1 = x_o,$$

which is as expected. This is nothing more than the mean position of the Gaussian centre.

The second cumulant is

$$\kappa_2 = 2Dt,$$

where the factor 2 here comes from the factorial factor in the denominator of the cumulant generating function. From this, the second moment is calculated as

$$\mu_2 = \kappa_2 + \mu_1^2 = 2Dt + x_o^2.$$

Finally plugging the results for the first and second moment back, one finds the representation of MSD.

$$\langle (x(t) - x_o)^2 \rangle = 2Dt$$

Similarly, in a three dimensional case, the relation between mean squared displacement and diffusion coefficient can be derived as

$$\langle (x(t) - x_o)^2 \rangle = 6Dt.$$

Chapter 3 Material and method

3.1 Introduction

This chapter describes the materials used and the experimental conditions and procedure carried out.

3.2 Lambda DNA

Lambda DNA (N3011L) was obtained from New England Biolabs (NEB). This duplex DNA is isolated from bacteriophage lambda (*c*I857 *ind* 1 *Sam* 7). The phage is isolated from the heat-induced lysogen *E. coli* λ cI857 S7. The DNA is finally isolated from the purified phage by phenol extraction and dialyzed against 10 mM Tris-HCI (p.H 8.0) and 1mM EDTA. This Lambda DNA is 48,502 base pairs in length and has a molecular weight of 31.5×10^6 Daltons.

Lambda DNA is a long and fragile molecule and thus to keep it stable it must be kept in an ideal chemical environment. Commonly, DNA molecules are sensitive to ionic strength and pH of the storage buffer. In addition, contaminant enzymes or reactive radicals may damage the DNA. Therefore when working with DNA, it is extremely important that buffers and any apparatus that comes in contact with the DNA (e.g. pipette tips), are autoclaved and wipe clean with ethanol before use. In order to avoid experimenter contamination, gloves should be donned at all times when handling any chemicals. Furthermore, when pipetting DNA from stock, shear force due to the

parabolic shape of the pipette tip may fragment the DNA molecule. This is because different parts of the DNA molecule flow into different stream lines of the parabolic liquid flow profile in the pipette tip. If the flow is too high, these shearing forces may fragment the DNA molecule. Thus, when the DNA solution is sucked in or ejected from the pipette tip, it must be carried out as slowly as possible to prevent accidental breaking of the long and fragile DNA molecule.

3.3 TE buffer

The buffer used for this experiment is Tis-EDTA (TE). This type of buffer has a high buffering capacity and has become a standard buffer of choice in DNA experiments.

TE buffer has two components. Tris(hydroxymethyl)Aminomethane (Tris#161-0719) is a primary amine and thus undergoes the reactions associated with typical amines. Tris (hydroxymethyl)aminomethane).was obtained from Bio-Rad.

The second component is EDTA (ethylenediaminetetraacetic acid) and it prevents DNA degradation by scavenging divalent metal ions. These ions are necessary for the functioning of many enzymes. EDTA was obtained from First BASE Laboratories. The TE buffer was first prepared under higher concentration, 10x TE, by mixing 10 mL Tris/HCL, 2 mL 0.5M EDTA with 88 mL DI water. The pH of this buffer was adjusted to 8.0. The buffering agent with a pH value of 8.0 keeps DNA deprotonated and soluble in water. This concentration was later diluted to the required final concentration

The ionic strength of the buffer is important since it influences the effective width and persistence length of the DNA. [20]

3.4 Dialysing Lambda DNA with TE buffer

Concentrated stock Lambda DNA was first thawed from freezer at 65° C for 5 mins. Next, the PCR tube of concentrated stock DNA was removed from heat bath and immediately placed under running water for 5 mins. Care was then taken when pipetting from the stock DNA to prevent damaging the molecules by unduly exerting large shear forces on the molecules while travelling up the fine pipette tip [31, 8]. The diluted DNA was then dialysed with Tris-EDTA (TE) buffer to obtain the final concentration.

3.5 Staining of Lambda DNA with YOYO-1 dye

The diluted DNA was next stained with fluorescent dye YOYO -1 (491/509 nm), from Invitrogen, at a binding ratio of one dye molecule per four base pair (4:1, b/dye). At this binding ratio, the DNA would be fully coated thus allowing it to be clearly visible during investigation. The stock fluorescence solution was diluted with the required TE buffer concentration to obtain the final dilution. The mixture containing YOYO -1 dye and TE buffer was covered in aluminium foil (to keep it light tight) and heated in a heat bath at 50 °C for 30 mins. The aluminium foil helped to reduce photo-bleaching of the dye. Next, the light tight PCR tube was removed and placed under running water for 5 mins. Lastly, the light tight PCR tube was placed in the refrigerator for at least 24 hours to allow the dye to intercalate with Lambda DNA.

3.6 Final sample preparation

In this experiment, three different buffer concentration were used; 1 x dilution of TE (10mM Tris/HCL, 1mM EDTA (pH 8.0), 0.1 x dilution of TE (pH8.0) and 0.01 x dilution of TE (pH8.0).

For the 1 x TE buffer conditions, the Lambda DNA sample was diluted with TE buffer and the DNA concentration was adjusted to 0.5 g/L. Next, the sample was diluted to 0.003 g/L. Finally the diluted DNA sample was labelled with YOYO-1. The dye base pair ratio was 4 base pairs per YOYO-1. After labelling, the DNA solution was placed in the refrigerator for at least 24 h to allow for full intercalation. The labelled DNA was further diluted into 0.006 g/L before placement into nanochannels so that single molecules can be easily observed.

3.7 Micro- and Nano-channel fabrications

The nanochannel circuit was first fabricated on a silicon (Si) wafer stamp. This allowed for multiple use of the Si stamp, via polydimethylsiloxane (PDMS) casting [32-34].

The Si stamp was first made at the Centre for Ion Beam Application (CIBA) on Hydrogen Silsequioxane (HSQ) photo-resist with the aid of a proton beam writer. A 3.5 MV High Voltage Engineering Europa B.V.(HVE) singletron accelerator is coupled to a nanoprobe end station. This

system is capable of focusing a proton beam down to 13x30 nm^2 spot size. This allows for the writing of the nanochannels for single molecule DNA analysis.

First the Si wafers are pre-coated with Chromium (Cr) and Gold (Au). Next, photoresist layers of HSQ XR1541 (60 and 105 nm thick layers) and FOX 12 (300 nm thick layer) were spin coated onto the Si wafers and next baked at 150°C for 120 s. After this preparation, parallel channels were written with proton beam, shown in Fig 3.7a below.

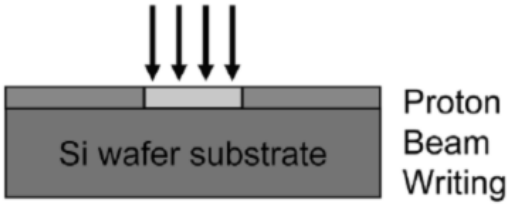

Fig 3.7a Proton Beam Writing

Through proton beam exposure the HSQ resist forms a cross-linked network that cannot easily be removed using chemical etching. After proton beam exposure, the samples were developed in a 2.38% tetramethyl ammonium hydroxide etching solution for 60 s removing the non-exposed parts, followed by a deionized water rinse and during this process the non-exposed parts were removed. Finally the moulds containing nanochannel structures were baked at 150 °C for 30 mins to harden the mould.

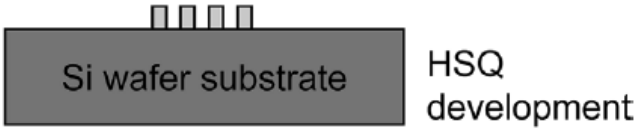

Fig 3.7b HSQ development

On top of the HSQ nanostructure, fig. 3.7b above, a microstructure channel linking the reservoir to the nanochannels was manufactured using SU-8. SU-8 is a negative tone photoresist material based on an epoxy resin. Under UV exposure the SU-8 molecules form a highly cross-linked network in the presence of a photo-inhibitor. The cross-linked network cannot be removed by a developer. Due to its low optical absorption, SU-8 can be patterned using optical lithography to a thickness of hundred micrometres with very high aspect ratios.

On the other hand, for the substrate, it is possible to use the described stamp above to carry the HSQ nanostructure. By the combination of the two different lithography processes, i.e. one in HSQ with proton beam writer and another in SU-8 with UV radiation, it is possible to produce a stamp with a (positive) microstructure superposed on an underlying nanostructure. The microchannels help to direct the DNA into the nanochannels from the relatively large reservoir.

The first stage of the UV-radiation lithography process involves pre-heating the sample at150 °C for 2 mins. Next a 5 μm thick SU-8 layer was spin coated at 2000 rpm for 30 s and exposed to a masked UV radiation. The SU-8 coated substrate was then baked on a hot plate at 95 °C for 120 s to fully crosslink the exposed molecules. The microchannels could be easily aligned to the underlying structure due to the low optical absorption of SU-8, shown below in fig 3.7c. Next, the SU-8 coated substrate was then post-baked on a hot plate at 95 °C for 120 s. The SU-8 was developed in a SU-8 developer for 120 s followed by a quick rinse with isopropyl alcohol (IPA), then rinse with deionized water and eventually drying with a gentle flow of dry nitrogen gas. Finally, the mould containing nano and micro-structures were backed at 150 °C for 30 mins to harden the mould.

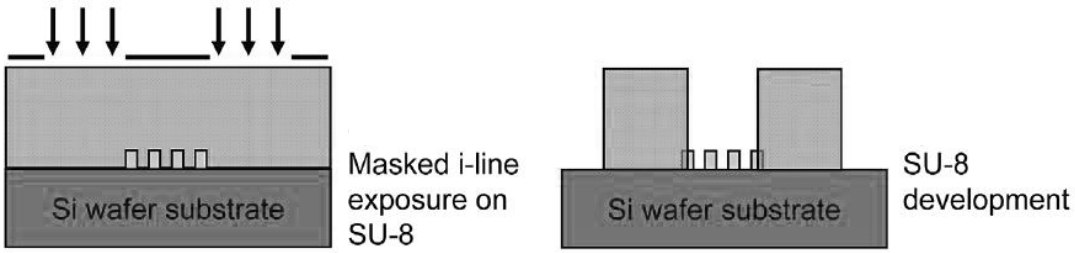

Fig 3.7c SU-8 development

In this experiment, two different nanochannels sizes were used; 300 x 300 nm^2 channels and 250 x 250 nm^2 channels.

3.8 PDMS casting

To produce the micro/nano-fluidic chip, the Si stamp described in the last section, was replicated by using polydimethylsiloxane (PDMS). The PMDS (SylgardTM 184 Silicone Elastomer Kit) was obtained from Dow Corning Corporation. The kit includes a liquid silicon rubber base (vinyl-terminated PDMS) and a catalytic curing agent (mixture of a platinum complex and copolymers of methyl-hydrosiloxane).

The PDMS base and curing agent are mixed at a ratio of 10:1 and blended to facilitate the dissolution of the catalyst into the base polymer. Mixing the base and curing agent of PDMS invariably

incorporates air bubbles into the polymer. These bubbles were removed after degassing the sample under a vacuum pressure of ~1 Torr for 30 mins. The gas free PDMS mixture was next poured onto the HSQ/SU-8 Si stamp wafer in a disposable weighing boat, shown below in Fig 3.8a. This sample was again degassed for a 30 mins to remove any further air bubbles trapped inside the PDMS. The PDMS pre-polymer was then allowed to cure by placing in an oven heated to 65 °C for 4 h. The cured PDMS was then carefully peeled with the aid of tweezers, moving from the outer edge of the Si stamp inwards. The separated PDMS structure was next inspected under an optical microscope to check of the micro/nano-structures are clearly defined and channels were not broken. The separated PDMS was then cut to size after reservoir access holes (1 nm diameter) were made using a needle punch (Harris Uni-Core, Jed Pella Inc.)

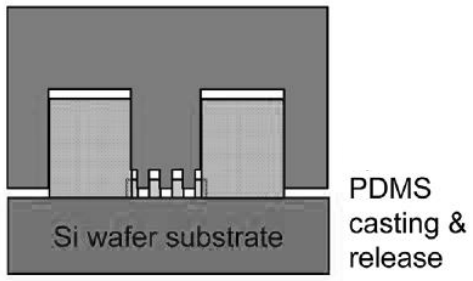

Fig 3.8a PDMS casting and release

Finally the PDMS micro/nano-channel device was bonded to a glass slide to allow the final device to be fluid tight. This critical step is important to provide a good seal; otherwise a leakage of fluid will exert high pressure on the fluid in the channel. This in turn will prevent any single DNA molecule to remain in the nanochannels for investigation. In order to enhance the seal between the PDMS and glass slide, the PDMS sample and glass slide were treated with air Radio Frequency (RF) plasma. Air

RF plasma treatment is effective in removing surface contaminants by roughening the bonding surface and chemically modifying surface groups. Thus air RF plasma treatment changes the surface from hydrophobic to hydrophilic, resulting in an oxidized PDMS surface resists absorption of hydrophobic and negatively charged molecules. This surface treatment usually last about 30 mins and this ultimately limits the time left for further steps. After this time, the hydrophobicity of the surface will recovered, regardless of whether the sample is in vacuum, air or water.

The PDMS sample and glass slide were pre-treated with air RF plasma for 30 s at a pressure of-0.23 Torr. Upon removal from the RF plasma chamber, the PDMS sample was brought into contact with the glass slide immediately, thus ensuring a reliable bond, shown below in Fig 3.8b. The bonded PDMS sample and glass slide were next placed on a heated (90 °C) hot plate for 60 s to improve the adhesion between the two surfaces. Lastly, the reservoir access holes were filled with the required buffer within 10 mins of removal from the hot plate in order to not loose hydrophobicity. Once, in contact with the buffer solutions the chip remains hydrophilic for tens of hours. [35]

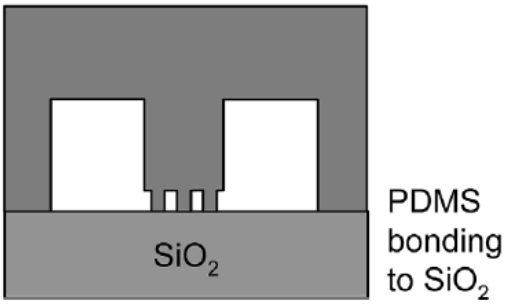

Fig 3.8b PDMS bonding to SiO_2

3.9 Video capture

Fluorescence microscopy uses fluorescence and phosphorescence instead of reflection and absorption to study the properties of organic and inorganic substances. The sample was illuminated with a light of a wavelength which excites the YOYO-1 dye within the sample. The emitted fluorescence light was then imaged through a microscope objective. Typical fluorescence microscope contains the excitation filter and emission filter which are chosen to match the spectral excitation and emission characteristics of the fluorophore use to label the specimen [36].

The stained DNA molecules in the relevant buffer solutions were injected into the two reservoirs in the PDMS cast at the two ends of the micro/nano channels. An electric field was used to help drive the DNA molecule through the nanochannels for analysis. This was done with the aid of platinum electrodes that were immersed into the two reservoirs and connect (at the other end) to an electrophoresis power supply with a voltage in the range of 0-10 V (Keithley, Cleveland Ohio), shown below in Fig 3.9. Once the DNA molecule were in the nanochannels and if the fluid pressure was balanced at both ends of the reservoir, then the DNA molecule would stay in the nanochannel for minutes during video capture. Unequal fluid pressure in both reservoirs would cause drift of the DNA molecule. Additional TE buffer could be injected into the reservoir using a small syringe to supress this drift after the same hydrodynamic pressure was maintained in both reservoirs.

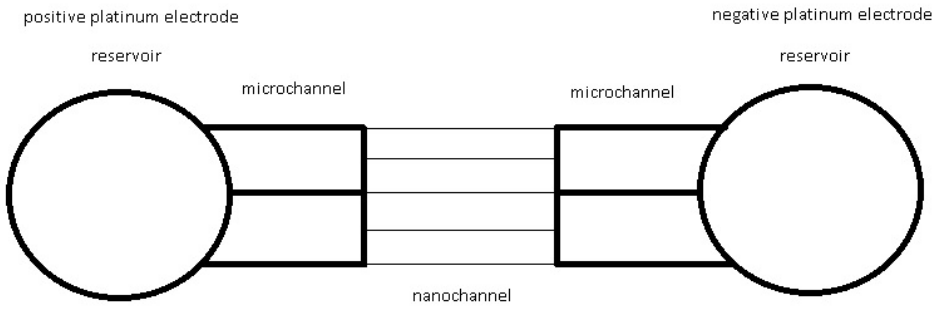

Fig 3.9 Nanfluidic system. (Top view of the two platinum electrodes immersed into the two reservoir, allowing for DNA molecules to be driven into nanochannels by electric field.)

The DNA molecules in nanochannels were visualised using a Nikon Eclipse Ti inverted fluorescence microscope, which is equipped with a 200 W metal halide lamp, a UV filter set and observed by a 100x oil immersion (NA 1.0 Nikon) objective. The microscope was coupled to a cooled back-illuminated EMCCD camera (Andor Technology, iXon X3). Image contrast was enhanced using Dark-Field microscopy. This works by illuminating the sample with light that is collected by the objective lens but as compared to an ordinary microscope, here only the light scattered by the sample is used to produce the image.

The exposure time of the spectrum was controlled by a UV light shutter. Images were collected by an electron multiplying charge coupled device (EMCCD) camera (AndoriXon X3) and displacement of

the DNA molecules inside the nanochannels were later measured using imageJ software. The electric field was switched on to direct the DNA molecule into the nanochannel for imaging and to change this DNA molecule with another for the next analysis. The frame rate was set at 31.23Hz during video capture.

3.9.1 Setup of CCD

The program Andor SOLIS was used to record the video after it was captured from the CCD camera, while the program NIS-Elements BR was used to control the camera. First, NIS-Element BR was used to find the location of the nanochannels, then the program Andor SOLIS was used to capture the image. Exposure time was set to 31.23 Hz, shown below in fig 3.9.1. The size of the video was set as 512 pixels x 512 pixels. The movie files were saved as tagged image file (.tif) format.

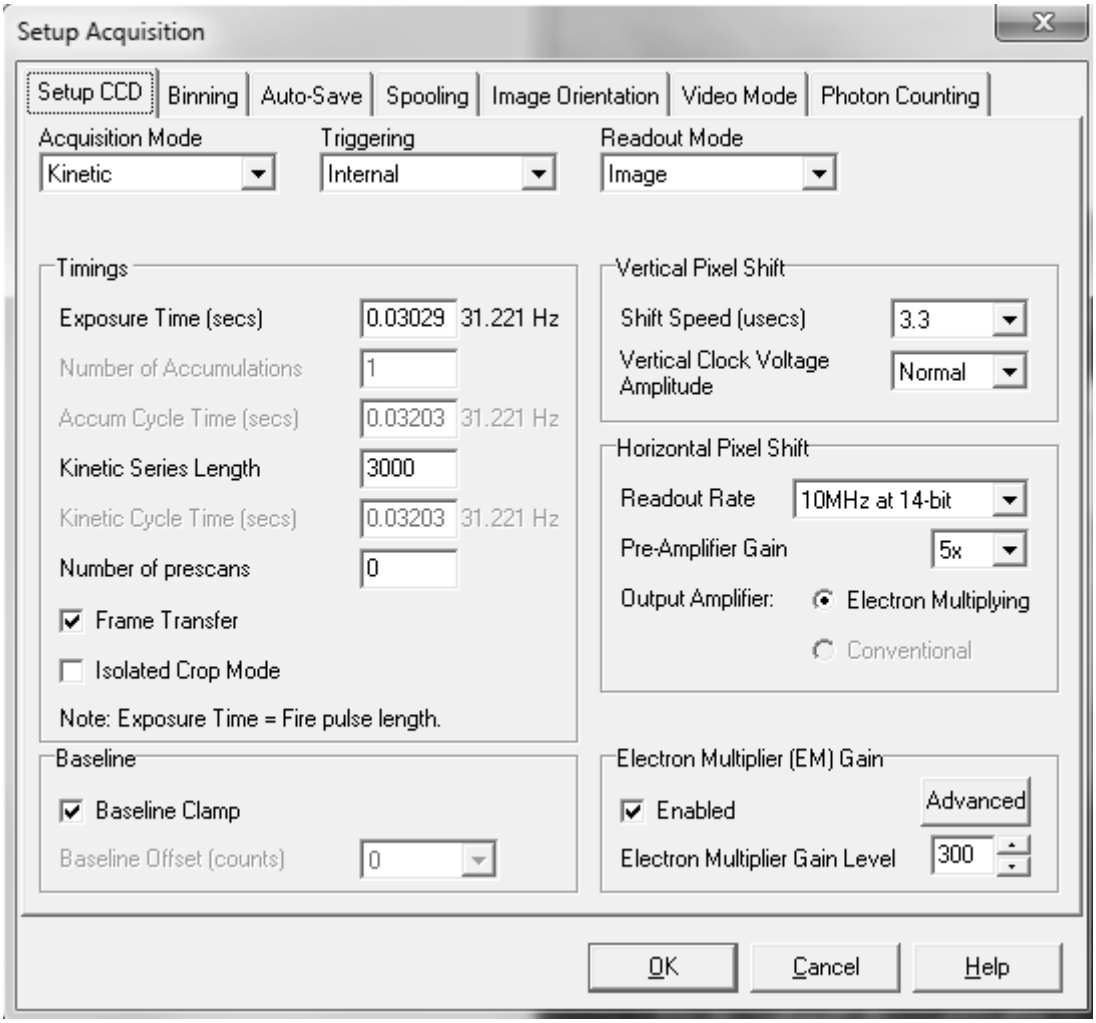

Fig 3.5.1 Setup of Andor SOLIS

3.10 Data cleaning

The movies were recorded by the Andor SOLIS and then analysed by ImageJ (image processing program) freeware. ImageJ was used to select (cut a box around a single DNA molecule), then rotate DNA molecule in a nanochannels for further analysis. Stuck, fragmented and double DNA molecules

stuck end to end were discarded from further analysis. Finally, the movie files were analysed using an in-house MATLAB program (described in the next section).

Using MATLAB, mean, minimum and maximum extension values of each DNA molecule were obtained to again reject fragmented, double DNA molecules stuck end to end and DNA molecules stuck in nanochannels. Fig 3.10a below shows the extension of YOYO-1 labelled Lambda DNA molecules in 1x TE buffer after data cleaning. All other data sets showed similar plots after data cleaning.

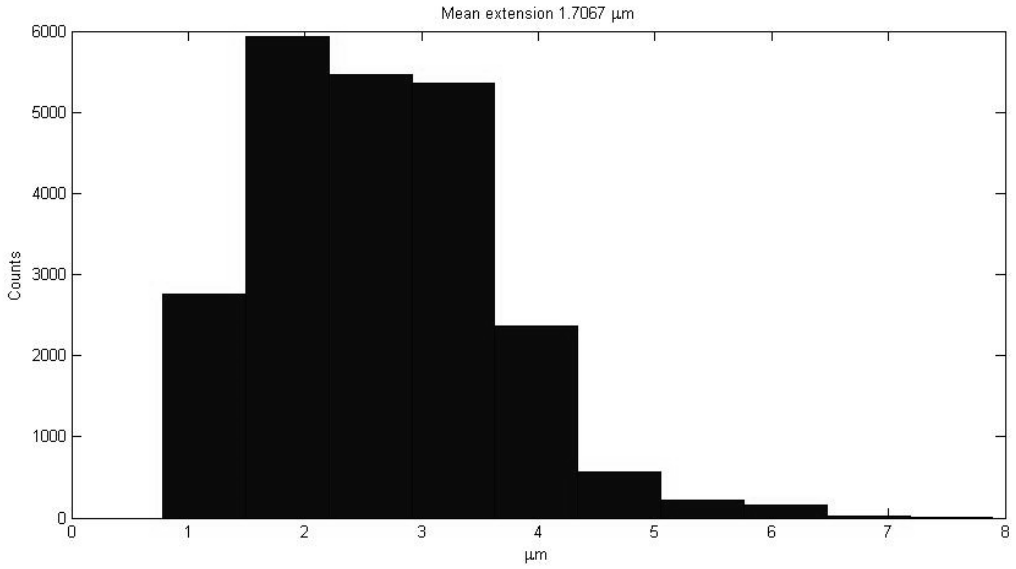

Fig 3.10a Distribution of the extension of YOYO-1 labelled Lambda DNA molecules in 1x TE buffer in a 300x300 nm^2 channel

Fig 3.10b below shows the extension of YOYO-1 labelled Lambda DNA molecules in 0.01x TE buffer after data cleaning.

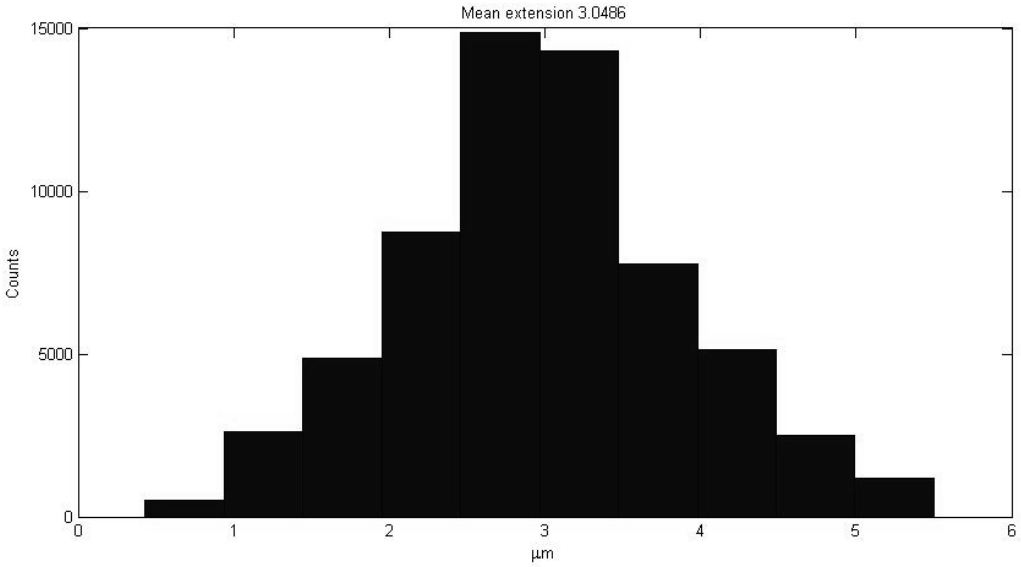

Fig 3.5.2b Distribution of the extension of YOYO-1 labelled Lambda DNA molecules in 0.01x TE buffer in a 300x300 nm^2 channel

Comparing fig 3.2.5a and fig 3.5.2b, the effect of reducing the TE buffer from 1x TE to 0.01x TE is clearly seen by the increase of mean extension from 1.7 to 3.0 µm. This would equate to an extension multiple of 1.8 times in the reduction in TE buffer concentration from 1x TE to 0.01x TE buffer.

Autocorrelation of time series data for each molecule's data set was further analysed for self-correlation. Final analysis included an average of 80 +/- 25 different DNA molecules for each experimental sample.

3.11 MATLAB program

The movies of single DNA molecules were then analysed by an in-house MATLAB program. Several programs were used during the analysis. Here, these programs are named as program A, B and C for brevity and convenience.

First, program A was used to determine the position of the molecule. In the method of YOYO-1 labelling, the intensity of each pixel on the DNA molecule in the movie was hypothesised to be proportional to the centre of mass at the corresponding position of the recorded molecule. The brighter the YOYO-1 signal observed proportionally equated to more binding sites that were able to bind YOYO-1, hence the greater the concentration of mass in that segment. Therefore, the equation,

$$r = \frac{\sum m_i r_i}{\sum m_i}$$

can be used to calculate the centre of mass of the particle in each frame; by changing the mass m_i that is located in space with coordinates r_i into the light intensity located at the same coordinate.

The output of the centre of mass analysis was a MATLAB mat file. This file contained data representing the movement of the centre of mass of each DNA molecule with its time evolution. Next, to help increase statistical reliability, all data files from the same experiment were merged into

a single larger file. This resulted in greater reliability in data analysis as when compared to analysing from just a single DNA molecule.

In program B, these larger files were analysed to obtain the mean squared displacement (MSD) of a single experiment. Program B counts the distribution of their relatively position of the DNA molecules with time. Next a Gaussian function was used to fit the distribution of the DNA molecules. The Gaussian function of the probability density function is derived from the diffusion equation. The diffusion equation states that the speed at which the probability of finding the particle at x(t) is position dependent.

$$P(x,t) = \frac{1}{\sqrt{2\pi < \Delta x^2 t >}} exp\left(-\frac{|x - x_o|^2}{2 < \Delta x^2 t >}\right)$$

Here $< (x - x_o)^2 >$ is the MSD, x(t) is the position of the particle with time and x_o represents the original position of the particle at t=0. This states that the probability of finding the particle at x(t) is Gaussian (shown below in fig 3.11), and the width of the Gaussian is time dependent. More specifically the Full Width at Half Maximum (FWHM) scales like FWHM $\sim\sqrt{t}$. Therefore the width of this Gaussian is proportional to MSD. The width of this distribution will broaden and the MSD of the molecule can be determined from the Gaussian distribution with time.

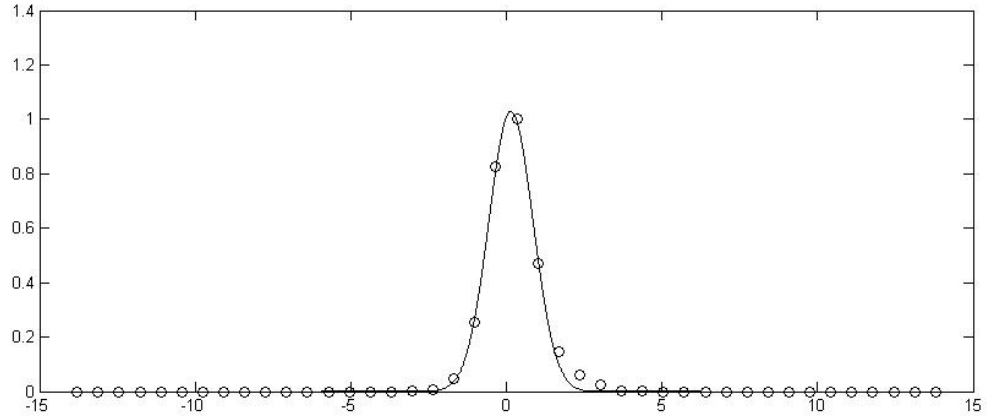

Fig 3.11 Gaussian fitting of probability density function to the measured position of DNA molecules in1x TE buffer in a 300nm x 300nm channel. X axis represents position and Y axis represents the distribution normalised to 1

As the DNA molecule in nanochannels only move in one axis of one dimension, the MSD data in one axis is used to plot the profile of MSD over time. Lastly, program C was used so as to fit the MSD data to obtain the diffusion coefficient results. As the relation between the squared displacement and diffusion coefficient is $< x - x_o >^2 = 2Dt$ (where D is the diffusion constant with S.I. units $m^2 s^{-1}$), the fitting curve should be a straight line that extended over time. Then the diffusion coefficient could be calculated from the slope of the straight line fit.

Chapter 4 Results and discussion

The experiment in this report involves first diffusing YOYO-1 labelled Lambda DNA into microchannels, and second to optically observe the fluctuations of these single molecules. Last is to analyse the mean squared displacement (MSD) of a statistically significant batch of molecules from the same experimental conditions. Two different channel dimensions are used, namely, the 300x300 nm^2 and 250x250 nm^2 nanochannels. In the wider 300x300 nm^2 microchannels, it can be hypothesised that the Lambda DNA molecules were free to move and their behaviour resembles that of diffusion. Further three different buffer concentration are used, namely, 1x TE, 0.1x TE and 0.01x TE buffer. The effect of lowering TE buffer concentration (decreasing ionic strength) increases the extension of Lambda DNA, hence making them more 'stiffer' and thus inhibiting their free diffusion behaviour in nanochannels. The MSD calculation of single Lambda DNA molecules in 300x 300 nm^2 channel with the three different TE buffer concentrations is shown in Fig 4a below.

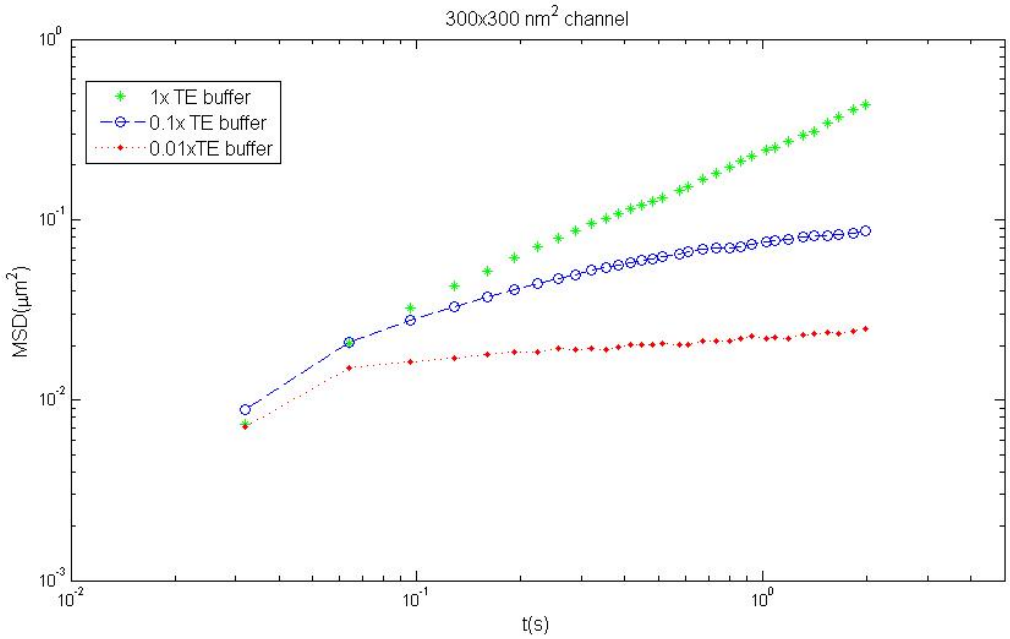

Fig 4a MSD of Yoyo-1 labelled Lambda DNA in 3 different buffer conditions in a 300x300 nm^2 channel

In fig 4a above, the YOYO-1 labelled Lambda DNA in 1x TE buffer shows near diffusion like behaviour. However, as the concentration of TE buffer is reduced, thus increasing the extension of the DNA molecule, the MSD data plot no longer has a slope of 1. This shows that for lower TE buffer concentrations, the Lambda molecule no longer exhibits diffusion like behaviour but now there is a flattening of the curve at later times. Further, the lower the TE buffer concentration the flatter the MSD curve. It is also interesting to notice from fig 4a above that at shorter times, the YOYO- labelled Lambda molecule does exhibit a diffusion like behaviour but soon after other effects take over, possibly the interaction between the stiffer Lambda DNA molecules and channel walls. Fig 4 b below shows the effect of a narrow channel diameter on YOYO-1 labelled DNA molecule in these same buffer concentrations.

From the MSD data, both the diffusion coefficient and hydrodynamic radius of YOYO-1 labelled Lambda DNA molecules can be calculated. The results are shown below in table 4a.

	Diffusion coefficient (m^2/s)	Hydrodynamic radius (m)
YOYO-1 labelled Lambda DNA in 1x TE buffer in 300x300 nm^2 channel	1.4 +/- 0.3 $x10^{-13}$	1.8 +/- 0.4 $x10^{-6}$

Table 4a Diffusion coefficients and hydrodynamic radius of YOYO-1 Labelled Lambda DNA in 1x TE buffer in 300x300 nm^2 channel

In the second channel dimension, namely the 250x250 nm^2 channel, the Lambda DNA molecules were not able to move freely as compared to the 300x300 nm^2 channel. Again, three different buffer concentration are used, namely, 1x TE, 0.1x TE and 0.01x TE buffer. The effect of lowering TE buffer concentration (decreasing ionic strength) increases the extension of Lambda DNA, hence making them more 'stiffer' and thus inhibiting their free diffusion behaviour in nanochannels. It is interesting to next investigate the effect of the narrower channel compared to the stiffening of the YOYO-1 labelled Lambda DNA molecule. The MSD calculation of single Lambda DNA molecules in 250x 250 nm^2 channel with the three different TE buffer concentrations is shown in Fig 4b below.

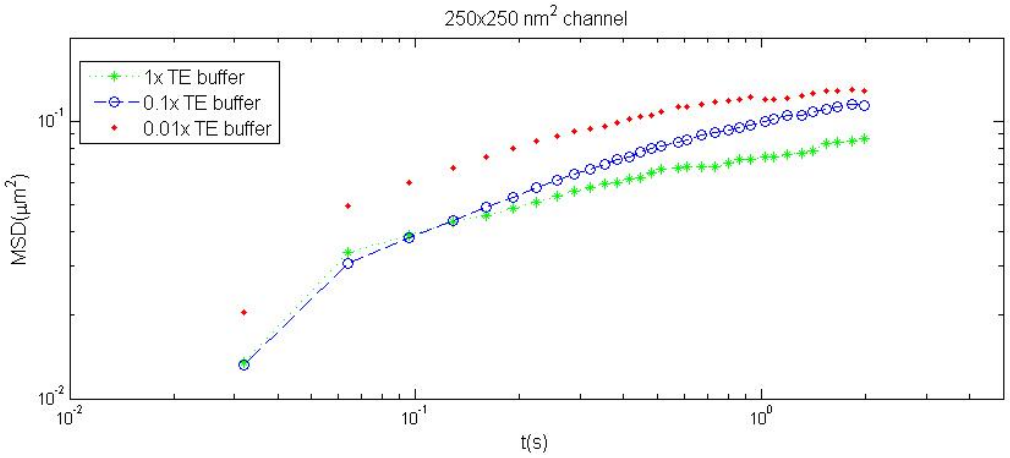

Fig 4b MSD of Yoyo-1 labelled Lambda DNA in 3 different buffer conditions in a 250x250 nm^2 channel

In fig 4b above, the YOYO-1 labelled Lambda DNA in all TE buffer concentration do exhibit near diffusion like behaviour initially. However, soon after, the MSD data plot no longer has a slope of 1, instead it levels off. This shows that for narrower channel dimensions the Lambda molecule no longer exhibits diffusion like behaviour but now there is a flattening of the curve at later times. Again, the effect of lowering the TE buffer concentration flattens the MSD plot.

In conclusion all the YOYO-1labelled Lambda molecules, except for the one in 1x TE buffer in a 300x300 nm^2 channel, do not have a slope of 1 in their MSD plots. Accordingly, it can be summarised that all these YOYO-1 labelled Lambda DNA molecules do not obey the diffusion law , except during the initial time in the analysis.

After the YOYO-1 labelled Lambda DNA molecule were moved into the nanochannels, an average of 3 minutes was given for the system to stabilise after switching off the electric field and before

starting the video recording. Therefore the initial time of the experiment would show the diffusion of the Lambda DNA in channels. If we look at the initial time of all the experiments, during which all the molecules have a slope of approximately 1, we are able to calculate the diffusion coefficients of these YOYO-1 labelled Lambda DNA molecules. By fitting only the first few data point, the behaviour is like a straight line of gradient 1. The fit curve of YOYO-1 labelled Lambda DNA in 0.1x TE buffer in a 300x300 nm^2 channel is shown in fig 4c below, and Table 4b below shows the diffusion coefficients obtained.

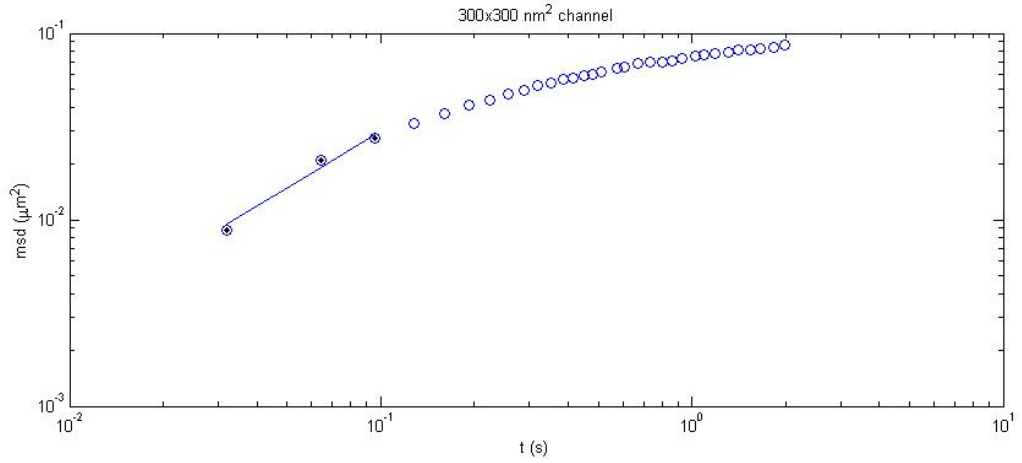

Fig 4c Fitting slope of diffusivity by using first three data points of MSD of YOYO-1 labelled Lambda DNA in 0.1x TE buffer in a 300x300 nm^2 channel.

	Diffusion coefficient (m^2/s)	Hydrodynamic radius (m)
YOYO-1 labelled Lambda DNA in 0.1x TE buffer in 300x300 nm^2 channel	1.4 +/- 0.2 x 10^{-13}	1.6 +/- 0.2 x 10^{-6}
YOYO-1 labelled Lambda DNA in 0.01x TE buffer in 300x300 nm^2 channel	1.4 +/- 0.05 x 10^{-13}	2.1 +/- 0.01 x 10^{-6}
	Diffusion coefficient (m^2/s)	Hydrodynamic radius (m)
YOYO-1 labelled Lambda DNA in 1x TE buffer in 250x250 nm^2 channel	1.2 +/- 0.4 x 10^{-13}	1.0 +/- 0.2 x 10^{-6}
YOYO-1 labelled Lambda DNA in 0.1x TE buffer in 250x250 nm^2 channel	1.2 +/- 0.2 x 10^{-13}	1.1 +/- 0.1 x 10^{-6}
YOYO-1 labelled Lambda DNA in 0.01x TE buffer in 250x250 nm^2 channel	1.2 +/- 0.5 x 10^{-13}	6.9 +/- 0.9 x 10^{-7}

Table 4b Diffusion coefficients and hydrodynamic radius of YOYO-1 Labelled Lambda DNA in nanochannels

The diffusion coefficient calculated above can still be used for analysis. In normal blob theory, the scaling law between the diffusion coefficient and height of slit should be $D \sim H^{2/3}$. This relationship can be written as $\log(D_2/D_1)/\log(H_2/H_1) = 2/3$. The calculated change of diffusion over the two channel diameters for the three buffer concentration is shown in table 4c below.

	$\text{Log}(D_2/D_1)/\text{log}(H_2/H_1)$ (H_2 = 300 nm, H_1 = 250 nm)
YOYO-1 labelled Lambda DNA in 1x TE buffer	0.5911
YOYO-1 labelled Lambda DNA in 0.1x TE buffer	0.5806
YOYO-1 labelled Lambda DNA in 0.01x TE buffer	0.5890

Table 4c Quantitative relationship between the calculated diffusion coefficients and diameter of nanochannels at the three different buffer concentrations

All the above results in table 4-3 are smaller than the estimated 2/3.

Interestingly, the above results agree with a revisiting theory. In classic blob theory, the dimensionless pair correlation function used is

$$h(r) = c_1 r^{2/3} L_p^{-1/3} w^{1/3}.$$

Where c_1 is a prefactor, r is the radius, L_p is the persistence length and w is the width. While in the revisiting blob theory, the pair correlation is modified as

$$h(r) = \begin{cases} 2 & r < L_p/2 \\ c_1 r^{2/3} L_p^{-1/3} w^{-1/3} & r \geq L_p/2 \end{cases}.$$

Where $h(r)$ is the dimensionless form of the pair correlation function. This modified pair correlation function minimally affects the static properties of DNA in slits, such as the scaling of extension. So the calculation of contour length of blob, L_{blob} is broke into

$$L_{blob} = \int_0^{L_p/2} h(r)dr + \int_{L_p/2}^{H/2} h(r)dr.$$

This correlation is substituted into the derivation and this result in a diffusion coefficient that can be written as

$$D = D_1 + D_2 - D_3.$$

The D_1 term is the same as the classic theory that obeys the scaling exponent $D_1 \sim H^{2/3}$ while the $(D_2 - D_3)$ term shows $(D_2 - D_3) \sim H^0$. Note that $(D_2 - D_3)$ term is positive and independent of H; i.e. scaling exponent is less than zero. The mixing of the two scaling exponents $D_1 \sim H^{2/3}$ and $(D_2 - D_3) \sim H^0$, result in an apparent exponent less than $2/3$ and this qualitatively agree with the results calculated above in table 4-3[37].

Chapter 5 Conclusion

This report investigates the mean squared displacement of single YOYO-1 labelled Lambda DNA molecules. Two different TE buffer concentrations were used and the florescent labelled Lambda molecules were driven into two different sized nanochannels. The single molecules were observed using a fluorescence microscope and images recorded using an optical camera. All mean squared displacement data showed a diffusion slope at least during the first few seconds of recording. This result implies that at later times, other channel effects may be taking place. This entropic trapping effect of the DNA in channel leads to an elastic response so that the MSD levels off as a constant value.

Additionally, comparisons of diffusions coefficients to the extension of DNA molecules agree with the predicted revisiting blob theory.

References

[1] Harris, S. A., (2004),The physics of DNA stretching, *Contemporary Physics*, **45**, 1.

[2] Gunther, K., Mertig, M., Seidel, R., (2010) Mechanical and structural properties of YOYO-1 complexed DNA,, *Nucl. Acids Res*., **38**, 19, 6526-6532.

[3] Rye, H. S., Yue, S.,Wemmer, D. E., Quesada, M. A., Haugland, R. P.,Mathies, R. A. and Glazer,A. N. (1992). Stable fluorescent complexes of double-stranded DNA with bis-intercalating asymmetric cyanine dyes: properties of applications. *Nucleic Acid Res*, **20**, 2803-2812.

[4] Sischka, A., Toensing, K., Eckel, R., Wilking, S. D., Sewald, N., Ros. R and Anselmetti, D. (2005) Molecular mechanisms and kinetics between DNA and DNA binding ligands. *Biophys. J*., **88**, 1, 404-411.

[5] Murade, C. U., Subramaniam,. V., Otto, C. and Bennink, M. L., (2009) Interaction of oxazole yellow dyes with DNA studied with hybrid optical tweezers and fluorescence microscope. *Biophys. J.* **97**, 835-843.

[6] Valeur, B.,(2001) *Molecular Florescence: Principles and Applications*, Wiley-VCH Verlag GmbH.

[7] Reisner, W., Morton, K. J., Riehn, R., Wang, Y. M., Yu, Z., Rosen, M., Sturm, J. C., Chou, S. Y., Frey, E. and Austin, R. H. (2005) Statics and dynamics of single DNA molecules confined in nanochannels. *Phys. Rev. Lett*., **94**, 196101.

[8] Mikkelsen, M. B. L. (2008), *Dynamics of DNA in a nanostructure confined environment.*

[9] Van der Maarel, J. R. C., (2007) *Introduction to biopolymer physics*, World Scientific (2008

[10] De Gennes, P G, (1979), *Scaling Concepts in Polymer Physics* (Cornell University Press).

[11] Odijk, T. (1983) On the statistics and dynamics of confined or entangled stiff polymers. *Macromolecules*, **16**, 1340-1344.

[12] Brochard, F., De Genne, P. G., (1977*)* Dynamics of confined polymers chains, *Journal of chemical Physics*, **67**, 52-56

[13] Zhang, C., Gong, Z. Y., Guttula, D., Malar, P.P., van Kan, J. A., Doyle, P. S. and van der Maarel, J. R. C. (2012) Nanouidic compaction of DNA by like-charged protein. *J. Phys. Chem. B*, **116**, 3031-3036.

[14] Schaefer, D. W., Joanny, J. F., Pincus, P. (1980) Dynamics of semiflexible polymers in solution, *Macromolecules*, **13**, 3, 1280-1289.

[15] Turban, L., (1984) Conformation of confined macromolecular chains: cross-over between slit and capillary, *Journal de Physique*, **45**, 2, 347-353.

[16] Flory, P. J., (1942) Thermodynamic of high polymer solutions, *J. Chem. Phys*., **10**, 51.

[17] Zimm, B. H.,(1956) Dynamics of polymer molecules in dilute solution: viscoelasticity, flow birefringence and dielectric loss, *Journal of Chemical Physics*, **24**, 269-278.

[18] Tree D.R., Wang, Y. and Dorfman, K. D. (2012) Mobility of a semiflexible chain confined in a nanochannel, *Phys. Rev. Lett.,* **108**.228105

[19] Mannion, J. T., Reccius C. H., Cross, J. D. and Craighead, H. G. (2006) Conformational analysis of single DNA molecules undergoing entropically induced motion in nanochannels. Biophys J., 90, 4538-4545.

[20] Reisner, W., Beech, J. P., Larsen, N. B., Flybjerg, H., Kristensen, A., Tegenfeldt, J. O., (2007) Single DNA molecules to changes in ionic environment, *Phys. Rev. Lett.,* **99**, 058302

[21] Jo, K., Dhingra, D. M., Odijik, T., de Pablo, J. J., Graham, M. D., Runnheim, R., Forrest, D. and Schwartz, D. C. (2007) A single molecule barcoding system using nanoslits for DNA analysis. Proc. Natl. Acad. Sci. U>S>A< 104, 2673-2678.

[22] Zhang, C., Zhang, F., van Kan, J. A., an van der Maarel, J. R. C.,(2008) Effects of electrostatic screening on the conformation of single DNA molecules confined in a nanochannel, J. Chem. Phys., 128, 225109.

[23] Kim Kim,Y., Kim,K.S., Kounovsky,K.L., Chang,R., Jung,G.Y.,dePablo, J.J., Jo,K. and Schwartz,D.C. (2011) Nanochannel confinement: DNA stretch approaching full contour length. Lab. Chip, 11, 1721–1729.

[24] Persson,F., Utko,P., Reisner,W., Larsen,N.B. and Kristensen,A. (2009) Confinement spectroscopy: probing single DNA molecules with tapered nanochannels. Nano Lett., 9, 1382–1385.

[25] Su,T., Das,S.K., Xiao,M. and Purohit,P.K. (2011) Transition between two regimes describing internal fluctuation of DNA in a nanochannel. PLoS One, 6, e16890.

[26] B. Kirby. (2010) *Micro- and nanoscale fluid mechanics: transport in microfluidic devices*. Cambridge University Press.

[27] Bonis-O`Donnell, J. T. D., Reisner, W and Stein, D. (2009). Pressure-driven DNA transport across an artificial nanotopography. *New Journal of Physics,* **11**, 075032.

[28] Mikkelsen, M. B., Flyvbjerg, H., Reisner, W., Kristensen, A. (2011). Pressure-driven DNA in nanogroves arrays: complex dynamics leads to length- and topology-dependence separation. *Nano Letters*, **11**, 1598-1602.

[29] Schoch, R. B., Han, J. and Renaud, P. (2008) Transport phenomena in nanofluidics. *Rev. Mod. Phys.*, **80**, 839-883.

[30] Berg, H. C.,(1993) *Random walks in biology*, (Princeton University Press).

[31] Reese, H. R., Zimm, B. H., (1990) Fracture of polymer chains in extensional flow: experiments with DNA and a molecular dynamics simulation, *J. Chem. Phys*., **92**, 2650-2662.

[32] Doyle, P.S., Ladoux, B., Viovy, J. L., (2000) Dynamics of a tethered polymer in shear flow, *Phys. Rev. Lett*., **84**, 4769-4772.

[33] Dukkipati, V., Kim, J. H.. Peng, W. and, Larson, R. G.(2006) Protein-assisted stretching and immobilization of DNA molecules in a microchannel, *Nano. Lett*., **6**, 2499-2504.

[34] Van Kan., J. A., Zhang, C., Malar, P. P., Van der Maarel, J. R. C., (2012) High throughput fabrication of disposable nanofluidic lab-on-chip device for single molecule, *Biomicrofluidics*, **6**, 036502.

[35] Hong, S. M., Kim, S. H., Kim, J., H., Hwang, H. I., (2006) Hydrophilic surface modification of PDMS using atmospheric RF plasma*, J. Phys. Conf. Ser*., **34**,656-661.

[36] Spring, K R, Davidson, M W., (2005) Introduction to fluorescence microscopy, http://www.microscopyu.com/articles/fluorescence/fluorescenceintro.html

[37] Liang. D., Douglas, R. T.,Van der Maarel, J. R. C., Dorfman, K. D. and Doyle, P. S. (2013) Revisiting blob theory for DNA diffusivity in slitlike confinement, *Phys. Rev. Lett*., **110**, 168105.